Whole-Range Finite Element Analysis of the Retrofitted Concrete Piers

Osamu ISHIBASHI[1], Hiroshi HIKOSAKA[2] and Guo-ping YANG[3]

1) M.Eng., Dai-ichi Fukken Consultants Inc., Fukuoka 812, Japan
2) Dr. Eng., Professor, Dept. of Civil Eng., Kyushu University, Hakozaki 6-10-1, Fukuoka 812, Japan
3) Ph.D., Guest Researcher from Tsinghua Univ., China; Dept. of Civil Eng., Kyushu University, Fukuoka

In the present paper, a reliable finite element procedure is developed to trace the whole-range structural responses of the reinforced concrete piers. In the computer code, a degenerate isoparametric curved shell element with layered model is adopted to simulate the out-of-plane structural responses. An arc-length algorithm combined with line search acceleration is employed to overcome the numerical difficulties near failure stage, and some important parameters affecting the performance of the algorithm are studied. With the proposed procedure, the structural responses of the concrete piers, with and without steel jacket retrofitting, are simulated up to softening stage. Based on the numerical simulations, the efficiency of the different retrofitting means is also discussed.
Keywords: Whole-range analysis, Arc-length method, Finite element, Concrete pier

1. Introduction

It is of first importance to evaluate the ultimate loading capacity of the concrete structures to be designed or already existed, and further to assess the earthquake resistance from the viewpoint of structural ductility (energy absorption ability). Some existing concrete structures are being stiffened since the big shock in Hanshin-Awaji area in January 1995, and many experimental investigations on steel jacket retrofitting of concrete bridge piers have been done by the Ministry of Construction, the Hanshin Expressway Public Corporation (noted as HEPC for short hereafter) and other organizations. However, these experiments are very expensive and unable to cover some other practical engineering situations, reliable numerical simulation therefore becomes an alternative.

The dynamic analysis of concrete structures demands the full-range response up to the softening stage. Finite element method has recently become the most powerful numerical tool in structural analysis through decades' development. But it is still very difficult to trace the full-range responses owing to the numerical instability and bifurcation near and post-failure stages. Near the ultimate load, a highly nonlinear structural response is usually encountered, stemming from concrete crushing and reinforcement yielding. Load control algorithms will inevitably fail to catch exactly the limit load, so many displacement control schemes have been proposed to pass the failure point[1-3].

Among the algorithms introduced into finite element analysis to trace the equilibrium paths, the arc-length method has given out some promising results[4-6]. Crisfield has done much successful work to improve the effectiveness of the method in solving softening problems. However, as pointed out by Crisfield[7], severe numerical difficulties have often been encountered when the arc-length method is applied to concrete structures, which usually leads to the abandoned solutions. A further research on arc-length method is necessary to improve the performance of the method, and most importantly, to get reliable and stable solution for concrete structures.

The present paper aims at tracing the full-range structural responses, from loading to the post-peak stage, of the reinforced concrete bridge piers. A degenerate isoparametric curved shell element with layered model is adopted to simulate the out-of-plane behavior. Both geometrical and material nonlinearities may be considered. The constitutive relationship of concrete includes the tensile and compressive softening branches. To overcome the numerical difficulties near and post-failure ranges, an arc-length algorithm combined with line search acceleration in the modified Newton-Raphson technique is employed, and some important parameters affecting the performance of the method, such as the value of the arc-length and the displacement

controlling increment, are studied. In each increment, the degree of the nonlinearity is monitored. If high nonlinearity is predicted, an increment size reduction is conducted to attain the convergence. With the proposed procedure, the whole-range structural responses of the concrete piers, with and without stiffening steel jacket, are simulated. The experimental results obtained from the HEPC are used to check the efficiency and reliability of our numerical simulations. Some other examples with different retrofitting means, not yet tested, are also computed to study the retrofitting mechanism and efficiency.

2. Layered Finite Element Formulation

The concrete piers to be simulated are in 3D stress states under the transverse horizontal forces. To simulate the out-of-plane structural response of the concrete piers, a degenerate isoparametric thick shell element with layered model is adopted, considering the real structural behavior and its key features. This thick shell element was proposed by Hinton and Owen[8]. In the formulation process, two approximations were used: the normals to the mid-surface remain straight after deformation and the stress component normal to the mid-surface is ignored. Each element contains eight nodes, and five degrees of freedom are used at each nodal point, corresponding to the three displacements and two rotations of the normal at the node.

A layered method is adopted to represent the varied nonlinearities across the shell thickness owing to the different materials and different deformation states. The specification of the layer thickness in terms of the curvilinear normal coordinate permits the variation of the layer thickness as the shell thickness varies. The element stiffness matrix k^e and the internal force vector f^e are simply defined as:

$$k^e = \iint_{-1}^{1} B^T D_{ep} B J d\zeta dA \qquad (1a)$$

$$f^e = \iint_{-1}^{1} B^T \sigma J d\zeta dA \qquad (1b)$$

in which B is the strain matrix calculated at the mid-surface of each layer, D_{ep} is the elasto-plastic material matrix, J is the determinant of the Jacobian matrix and σ is the stress vector at the integration Gauss point. The total number of the layers in the structure can be taken arbitrarily depending on the accuracy desired and the cost of the computation. In our examples, maximum 10 layers of concrete and 20 layers of reinforcements and hoops are adopted.

3. Material Models

The constitutive relationship of concrete includes the tensile and compressive softening behavior in terms of Fracture-plastic expressions, and linear elastic unloading mode is assumed for both tension and compression.

For concrete in tension, smeared crack model is adopted. The material behavior is assumed to be linear until the fracture surface is reached. Concrete cracking is controlled by a simple maximum tensile stress criterion. When the stress reaches the critical value, crack is assumed to form in the plane perpendicular to the direction of the maximum principal tensile stress. Then a linear softening model is assumed as shown in Fig.1[8], where the Fracture Energy is not adopted to connect the softening modulus with the mesh size. The fixed cracking direction is recorded, which means that the cracking direction does not rotate in the succeeding stress variation. A second crack is assumed to form perpendicular to this crack direction when the stress criterion is again reached. The shear retention of concrete in tension zone is also taken into account. In other words, the cracked concrete is simulated as an orthotropic material.

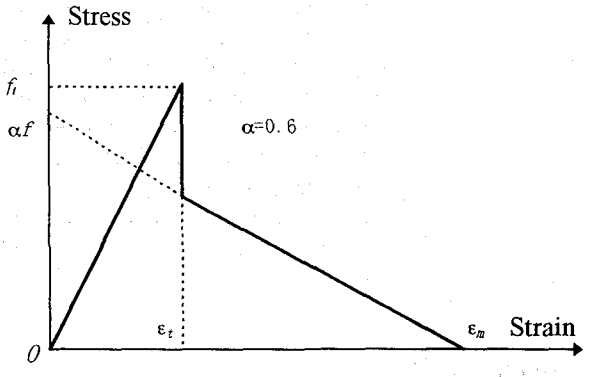

Fig.1 Effective stress-strain relationship of concrete in tension.

The concrete behavior in compression is supposed to follow the strain hardening rule of the plastic flow theory. The yield criterion is defined in terms of the first two stress invariants[8]

$$f(I_1, J_2) = \left[\beta(3J_2) + \alpha I_1\right]^{1/2} = \sigma_0 \qquad (2)$$

where I_1 is the first invariant of stress tensor, J_2 is the second invariant of stress deviator tensor, α and β are material parameters defined in Ref.8, and σ_0 is the equivalent effective stress, whose value will be taken from the ultimate stress for a uniaxial compressive test in our model. The associated flow rule is considered in the computer code. The concept of effective stress and effective plastic strain is also adopted to define the work hardening rule, softening behavior and crush condition. The hardening rule, softening branch and crush condition are related with the equivalent uniaxial stress-strain diagram in compression as shown in Fig.2.

The initial yield surface is attained when the effective stress reaches 30% of the peak compressive stress, then an isotropic hardening flow rule controls the material matrix.

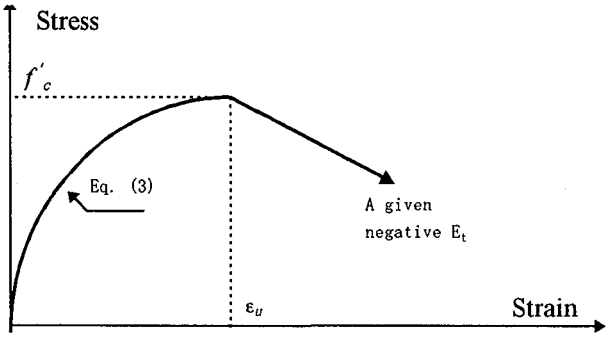

Fig.2 Equivalent uinaxial stress-strain relationship of concrete in compression.

After the effective stress reaches the peak strength, concrete is assumed working in the softening range, and crushing is assumed when the effective plastic strain reaches 0.0035 or a larger given value. The softening branch is governed by an input descending negative modulus E_t. The ascending part is assumed as:

$$\sigma^{ef} = f_c'(2x - x^2), \quad x = \varepsilon^{ef} E_o / (2f_c') \quad \text{for } f_c' < \sigma^{ef} < 0 \tag{3}$$

where σ^{ef}, ε^{ef} are effective stress and effective plastic strain, f_c' and E_o are peak compressive stress and initial Young's modulus, respectively. In both tension and compression, unloading is assumed to follow the secant modulus from the unloading point (linear unloading mode).

As for the reinforcements and hoops, they are all assumed to be distributed evenly in certain layers in the structure, and possess only stiffness in their longitudinal directions. This model is often used in practical structural analysis, while the retrofitting steel jacket is considered to be effective in both directions. Their stress-strain relationships are simplified as bi-linear approximations: when the yield stress is attained, the corresponding Young's moduli are reduced to 1 % of their original values.

4. Arc-length Algorithm Combined with Line Search Acceleration

In experimental investigations, full range response of concrete structures, from beginning to post-peak stages, can be obtained by displacement control mode. But it is very difficult to model this real existing process with finite element analysis[9-10]. This is mainly due to the presentation of the highly nonlinear response with large deformations near or beyond the peak load owing to the concrete crushing and reinforcement yielding. For example, negative tangential modulus, introduced from the strain-softening of the fracture mechanics of concrete for cracked concrete, has large effects on stability and uniqueness of the solution[11]. It is necessary to take this negative modulus into account, otherwise the computational results will depend on the mesh size.

Moreover, the concrete structures present 'snap-through' or 'snap-back' responses connected with strain localization and alternative equilibrium paths owing to the softening characteristics. Great effort has been conducted to trace the whole structural responses in nonlinear finite element analysis of concrete structures, but only little achievement has been obtained. The problem focuses on the suitable selection of the solving techniques. Near the peak loading, the global stiffness matrix will become ill-posed owing to the presence of some very small values or even negative pivot elements, and the condition number of the stiffness matrix is very large, which will give rise to a large solution error or make the equations unsolvable even though the structural displacements do have solution.

Among various candidate numerical methods, arc-length method with line search has been proved probably most successful for nonlinear analysis of the concrete structures near and beyond peak loads. However, the efficiency of the method in concrete structures encounter significant challenges. The iteration process often diverges or converges to an unreasonable solution[7]. So it is necessary to take advantage of this method and to obtain the reliable results, independent of the simple parameter choices such as the incremental size and mesh discretization.

Unlike the situations in load control procedures, a given value L, the arc-length, will set spherical constraint on the iteration path to find related load factor variation $\delta\lambda$:

$$\Delta \boldsymbol{u}_i^T \Delta \boldsymbol{u}_i + C\delta\lambda^2 \boldsymbol{q}^T \boldsymbol{q} = L^2 \tag{4}$$

in which $\Delta \boldsymbol{u}_i$ is the incremental displacement vector after $(i\text{-}1)$th iteration, $\boldsymbol{q}$ is the reference external load vector, and C is a constant related to the load vector. In Crisfield's work, C is set to be zero, so it is actually a generalized displacement control strategy.

The iterative displacement is

$$\Delta \boldsymbol{u}_{i+1} = \Delta \boldsymbol{u}_i + \eta_i \delta \boldsymbol{u}_i = \Delta \boldsymbol{u}_i + \eta_i (\boldsymbol{d}^* + \delta\lambda_i \boldsymbol{d}_T) \tag{5}$$

in which η_i is an acceleration parameter determined from line search (in the case of no line search, η_i=1), $\boldsymbol{d}^*$ and $\boldsymbol{d}_T$ are iterative displacement vectors corresponding to the residual and the reference loads, respectively. From the constraint in Eq.(4), a quadratic equation can be obtained to solve the load factor variation $\delta\lambda$:

$$a_1 \delta\lambda_i^2 + a_2 \delta\lambda_i + a_3 = 0 \tag{6}$$

in which:

$$\begin{aligned} a_1 &= \eta_i \mathbf{d}_T^{\mathrm{T}} \mathbf{d}_T \\ a_2 &= 2(\mathbf{d}_T^{\mathrm{T}} \Delta \mathbf{u}_i + \eta_i \mathbf{d}_T^{\mathrm{T}} \mathbf{d}^*) \\ a_3 &= 2\mathbf{d}^{*\mathrm{T}} \Delta \mathbf{u}_i + \eta_i \mathbf{d}^{*\mathrm{T}} \mathbf{d}^* \end{aligned} \tag{7}$$

The acceleration parameter η_i in the above equation should be determined from the stationary energy condition

$$\frac{\partial \Psi}{\partial \eta_i} = \frac{\partial \Psi}{\partial u}\frac{\partial u}{\partial \eta_i} = -r_{i+1}^T \delta u_i = S_j = 0 \tag{8}$$

where Ψ is the system energy. In numerical computation, it is difficult to meet the above equation, therefore an optimum slack condition

$$S_j < 0.8 S_o \tag{9}$$

is usually adopted[12]. So $\delta\lambda_i$ and η_i should be solved simultaneously to get the incremental displacement vector.

From the authors' computational experience, it is very important to choose the suitable value of the arc-length according to the degree of the nonlinearity encountered during the incremental process. When the norm of the incremental displacement vector or the loading point's displacement increment is less than a given value, the arc-length is taken as 1.256 times of the norm. While when the highly nonlinear structural response occurs, for example, the displacement increment for the same loading increment becomes 20 times more than that of the initial stage, a constant arc-length will be used to control the displacement increment. Moreover, the adoption of line search is necessary to get converged solution near the peak loading stage from these examples.

5. A Simple Example to Check the Whole Range Prediction Capacity of the Solver

To check the prediction capacity of our equation solver based on the arc-length method, a very simple example is computed. The model is a one-dimensional bar with four nodes and three elements as shown in Fig.3. Although this is an extremely simple example, it includes all respects in usual finite element analysis.

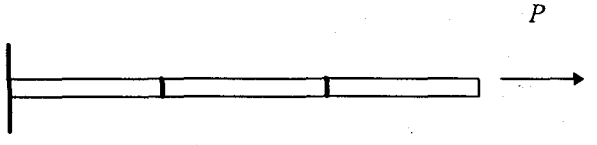

Fig.3 The simple example to check the equation solver.

The constitutive relationship is simply assumed as

$$\sigma = E^*(2\varepsilon\varepsilon^o - \varepsilon^2) \tag{10a}$$

$$E(\varepsilon) = \frac{d\sigma}{d\varepsilon} = 2E^*(\varepsilon^o - \varepsilon) \tag{10b}$$

With assumed parameters of square area A=100, length L=100, ε^o=0.0123456789 and Young's modulus E=20000, the computed maximum load is 304.775, very close to the exact maximum load 304.832. As a one-dimensional problem, theoretical displacement of the loading end can be simply obtained from the stress-strain relationship, ignoring the strain localization. The computed displacements are exactly the same as the theoretical ones, as shown in Fig.4. It can be seen from this example that the solver is able to trace whole range response with softening negative modulus.

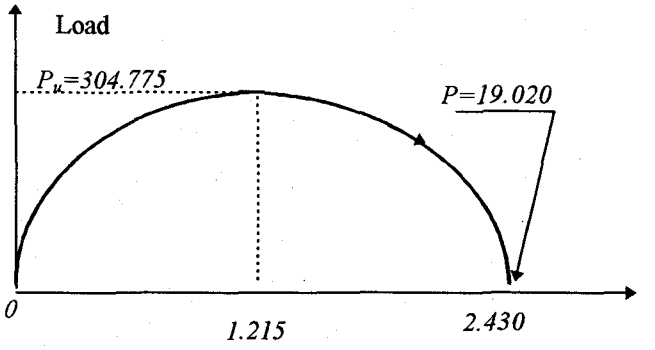

Fig. 4 Computed load-displacement relation.

6. Computational Examples of the Concrete Piers

Some reinforced concrete piers are computed with developed computer code. These piers include specimens with and without steel jacket retrofitting. The ultimate loads and deformations are compared by the experimental results from the HEPC[12] to check efficiency and reliability, and then some other cases not yet tested are computed to evaluate the effectiveness of the different retrofitting means. It should be noted that these piers are approximately modelled as thick shell structures, so the normal stress along the thickness direction and the 3D confining effects from both concrete and steel are not included. The geometrical nonlinearity is also not considered for these piers.

6.1 Examples with Experimental Results

The first example is a concrete pier named as No.1 for short, without retrofitting, see Fig.5(a) and Fig.5(b) for details. A transverse load is 3000 mm high from the base. The material parameters of concrete and steel bars are grouped in Tab.1 and 2, respectively.

Tab.1 Concrete parameters (kgf/cm^2)

Specimen	f'_c	f_t	E_c
No. 1	365	25.7	2.75*1^5
4H	295	23.0	2.58*1^5

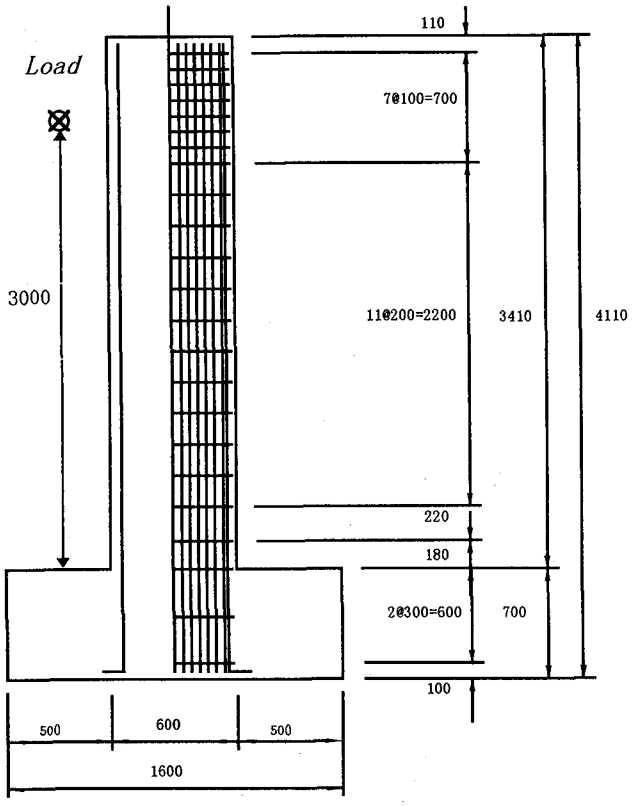

Fig.5(a) Elevation of the specimen No.1(mm).

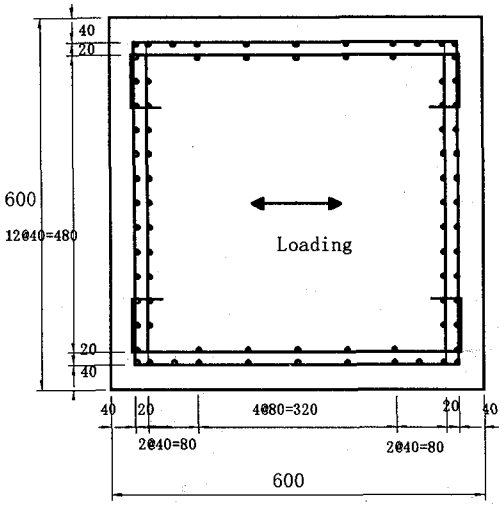

Fig.5(b) Details of the specimen No.1(mm).

Tab.2 Yield strengths and Young's moduli of the reinforcement and hoop (kgf/cm^2)*

Specimn	f_{yr}	E_r	f_{yh}	E_h
No. 1	3890	$1.81*10^6$	3343	$1.85*10^6$
4H	3704	$1.91*10^6$	3398	$1.92*10^6$

* r - reinforcement, h - hoop

A coarse mesh of 200mm*200mm is adopted as shown in Fig.5(c). The pier is divided into 3*17=51 elements, 194 nodes, 2 different patterns of layer, each pattern containing 8 layers of concrete and 15 layers of reinforcements and hoops. Total number of the degrees of freedom is 970.

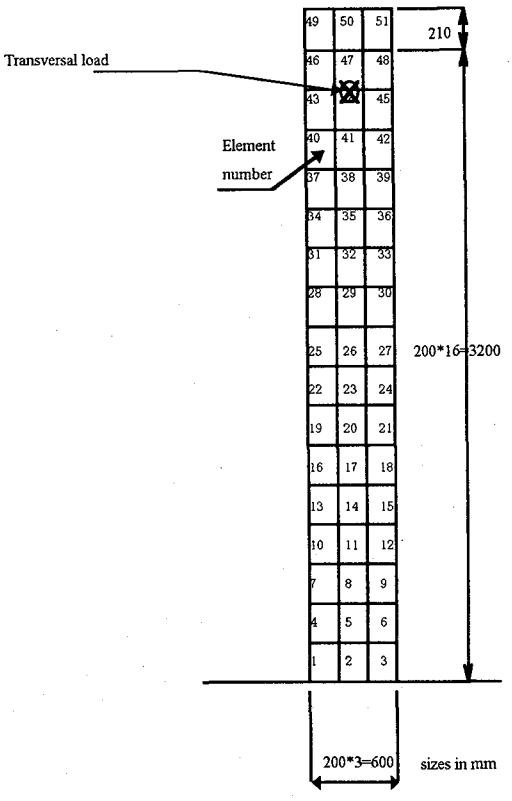

Fig.5(c) Finite element mesh of the specimen No.1.

The load-displacement curve of the loading point is shown in Fig.6. Computed ultimate load is 22.172 tf, compared with 22.8 tf from experiment, the relative error is 2.75%. A softening part with load level 20.892 tf is obtained.

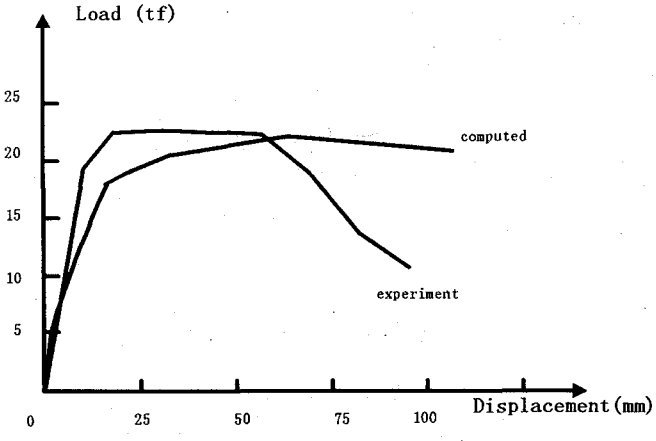

Fig.6 Load-displacement relations of the specimen No.1.

Since the experimental data of the stress are not at hand, only the computational variations of the stresses of concrete surface in compression and reinforcement in tension are shown in Fig.7 and Fig.8, respectively. The legends T5, T10, T14 and T15 are referred to the load

levels 8.114 tf, 16.583 tf, 21.172 tf and 20.892 tf, respectively. From Fig.7 and Fig.8, it is found that the variations of concrete compressive stress and the reinforcement stress along the height are nearly linear up to the load level 8.114 tf. With the increase of the load, the variations become steeper and steeper, which is corresponding to the localized deformations in the lower part of the pier. When the load increases from 8.114 tf to 16.583 tf, stress change rate of the steel bar is quicker than that of the concrete. The stresses of the steel bar decrease owing to the softening behavior of the structure.

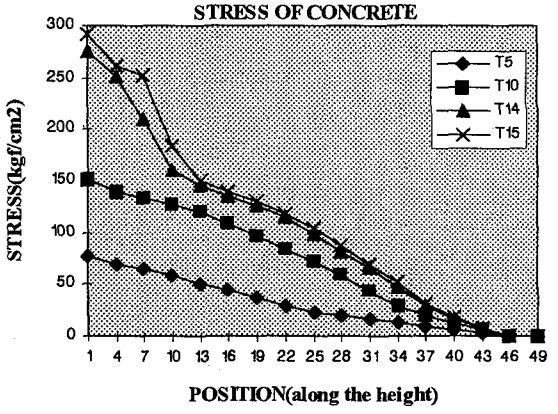

Fig.7 Compressive concrete stress variations along the pier height.

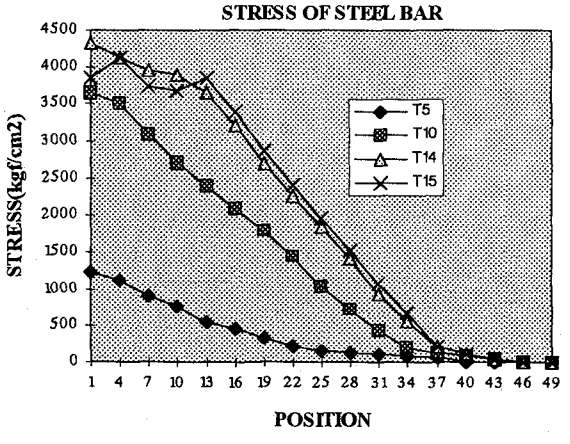

Fig.8 Tensile stress variations of the reinforcements along the height.

The second example is named as 4H, following the denotation from the HEPC. The details for steel jacket retrofitting are shown in Fig.9(a) and Fig.9(b). The thickness of the steel jacket is 1.6 mm, with yielding stress 2990 kgf/cm^2 and initial Young's modulus 2.14*10^6 kgf/cm^2.

It should be noted that there exists a gap of 50 mm between the steel jacket and the base, and the bottom of the pier is stiffened by reinforced concrete with height of 350 mm, whose major reinforcements are anchored into the base. The anchoring steel bars are 6 mm in diameter, with yielding stress 5133 kgf/cm^2 and Young's modulus 2.05*10^6 kgf/cm^2. In such a way, the steel jacket is not very effective in the connection between the pier and the base. In our computation, the contribution of the steel jacket is reasonably not included in considering the boundary conditions. The material parameters are also grouped in Tab.1 and Tab.2.

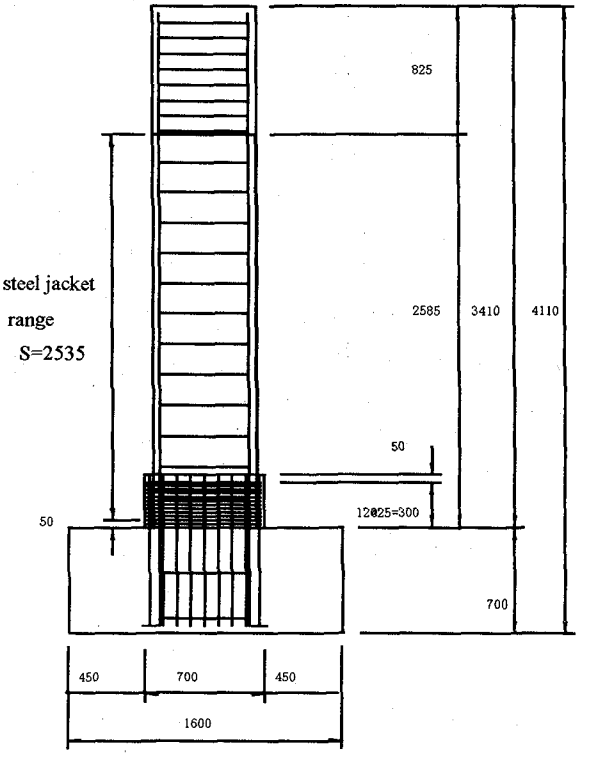

Fig.9(a) Elevation of the specimen 4H(mm).

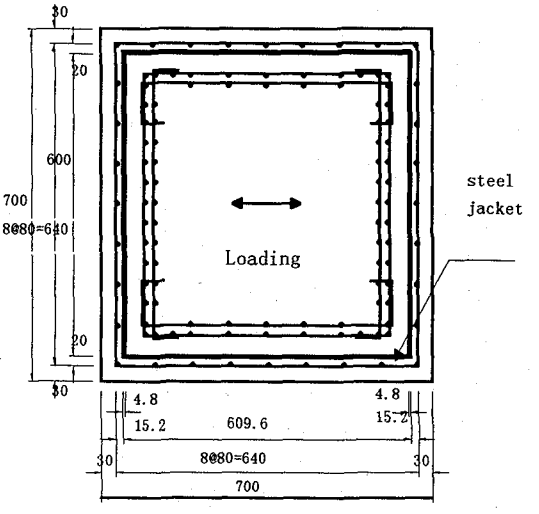

Fig.9(b) Cross section of the specimen 4H(mm).

The transverse load is also 3000 mm high from the base. The comparison of the load-displacement relation of the loading point is shown in Fig.10. It can be seen that the computed deformations, with part of softening branch corresponding to the load level 23.793 tf, are close to those from experiment. The computed ultimate load is 33.237 tf, compared with the experimental value 33.5 tf, the relative error is 0.785 %.

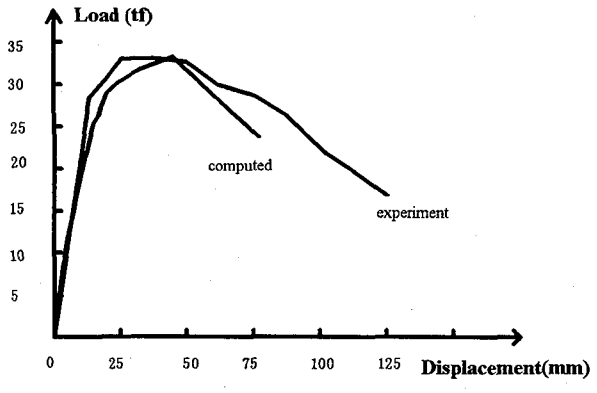

Fig.10 Load-displacement relation of the 4H.

The variations of the stresses of compressive concrete, tensile reinforcement and steel jacket are shown in Fig. 11, Fig.12 and Fig.13, respectively. The corresponding load levels are: T5=8.257 tf, T10=17.631 tf, T15=26.336 tf, T19=33.237 tf and T20=23.793 tf. In Fig.13, the stresses of the steel jacket in the lower stiffening element is not included. From these Figs, it can be found that the deformation localization is limited in the lower part of the pier. At the maximum load, concrete is crushed, and both of the jacket and main reinforcements are yielded.

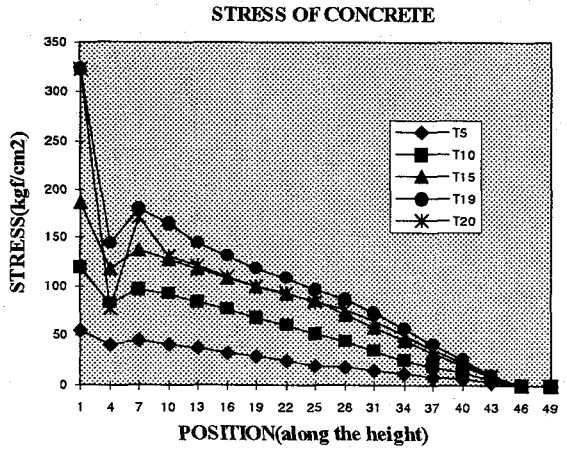

Fig.11 Concrete stress variations along the pier height.

In the softening branch, the stresses in the lower elements decrease sharply with the continuing deformation, and the deformation makes structure unloading. In real situations, this stage is usually accompanied with the local buckling of the compressive steel bars and the jacket.

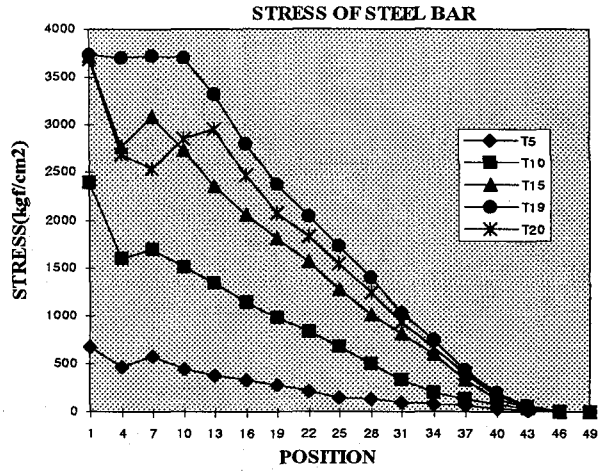

Fig.12 Tensile stress variations of the reinforcement along the pier height.

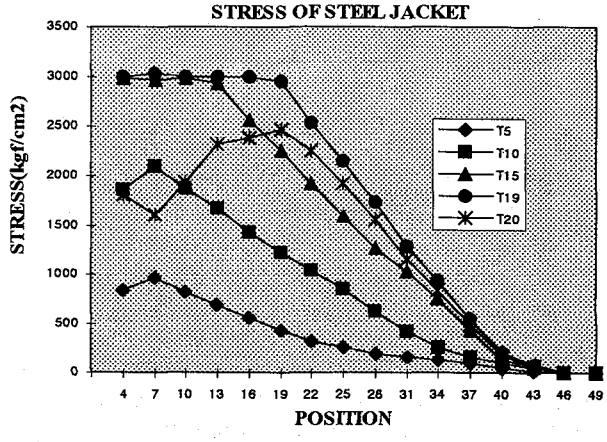

Fig.13 Tensile stress variations of the steel jacket along the pier height.

6.2 Other Examples not yet Tested

From the above examples, the reliability and efficiency of the computer code, especially the very good predictive ability for ultimate strength, have been verified. To study the retrofitting mechanism, some other examples with different stiffening means are also computed. These examples keep the same geometrical scalings of the specimen 4H, with only the lengths of the retrofitting steel jacket changed. The lengths and the corresponding predicted ultimate strengths are grouped in Table 3, in which S represents the length of the steel jacket.

From Tab.3, it can be found that the ultimate strengths

of the piers increase with the length of the retrofitting steel jacket, but the strengths with the jacket longer than 1414 mm are almost the same. These results show that the effectiveness of the length of retrofitting steel jacket is limited; when the length reaches a certain value, corresponding ultimate loads will not increase any more.

Table 3 Computed ultimate strengths (tf)*

No.1 without the jacket	No.4H1 only the lower RC stiffener	No.4H2 with jacket S=841	No.4H2 with jacket S=1414	No.4H2 with jacket S=1987	4H with jacket S=2535
22. 172	26. 275	32. 824	33. 204	33. 360	33. 327

* The length of the steel jacket, S, is in mm, see Fig.9(a) for details.

It seems that the extra length of the jacket beyond S=1414 mm is not necessary if only considering the ultimate strength. However, the termination of the main reinforcements at the mid-height in usual engineering practice will lead to the shear failure of the concrete piers[13], as occurred in great quantity in the 1995 Hanshin-Awaji earthquake. So it is suggested that a suitable jacket length should be used to meet the requirements that the weak part with inadequate main reinforcements should be stiffened.

7. Concluding Remarks

In the present paper, the arc-length method combined with line search is adopted to solve the whole structural responses of the concrete piers. Comparative research of numerical modeling and experiments on the piers shows the good ultimate strength prediction capacity of our newly developed software. Since it is only our first part of work, the effect of geometric nonlinearity, the most suitable constitutive relationship of concrete material and the buckling of the reinforcements and jacket are not included, which results in the partial capacity to trace the full softening response of the piers. An improvement will be conducted in the further research.

The effectiveness of the length of retrofitting steel jacket is limited. When the length reaches a certain value, corresponding ultimate loads will only change slightly in the case of enough anchoring length of the main reinforcements. However, considering the practical engineering situations, it is suggested that a suitable jacket length should be used to meet the requirements that the weak part with inadequate main reinforcements should be stiffened.

References

1) P.G. Bergan and R.W. Clough, Convergence criteria for iterative procedures, *AIAA Jn,* **10**, 1107-1108,1972.

2) M.J.Murray and G.J.Hancock, A study of incremental-iterative strategies for non-linear analysis, *Int. J. Num. Meth. Engng*, **29**, 1365-1391, 1990.

3) H. Park, R.E. Klingner and D.L. Wheat, Numerical techniques for predicting brittle failure of reinforced concrete planar structures, *J. of Strut. Engng.*, ASCE, **121**,1507-1513, 1995.

4) C.H. Sun, M.A.Bradford and R.I. Gilbert, A reliable numerical method for simulating the post-failure behaviour pf concrete frame structures, Computers & Structures, **53**, 579-589, 1994.

5) M.A. Crisfield, An arc-length method including line searches and accelerations, *Int. J. Numer. Meth. Engng.* **19**, 1269-1289, 1983.

6) M.A. Crisfield, Snap-through and snap-back response in concrete structures and the dangers of under-integration, *Int. J. Numer. Meth. Engng.* **22**, 751-767, 1986.

7) M.A. Crisfield and J. Wills, Solution strategies and softening materials, *Comput. Meths. Appl. Mech. Engng.*, **66**, 267-289, 1988.

8) E. Hinton and D.R.J. Owen, *Finite Element Software for Plate and Shells*, Pineridge Press Limited, Swansea, UK, 1984.

9) Guo-ping.Yang and H.M. Che, Experimental investigations on Partially Prestressed Concrete Box Girders, *J. of Bridge construction*, **20**, 1991 (in Chinese).

10) T. Tanabe, New advancement in concrete structural analysis, J. of Japan Society of Civil Engineers, **79**, 54-60, 1994 (in Japanese).

11) Guo-ping Yang and H.M.Che, Stability and Uniqueness in Analysis of Concrete Structures, *Proc. Intl. Symp. on Concrete Engng.*, Nanjing, 1991.

12) Hanshin Expressway Public Corporation, Model tests on steel jacket retrofitting of the damaged reinforced concrete piers, March, 1996(in Japanese).

13) K. Kawashima, J. Hoshikuma and S. Unjoh, A seismic evaluation method for reinforced concrete bridge piers with inadequate anchoring length at termination of main reinforcements, *J. of Structural Mechanics and Earthquake Engineering, JSCE*, No.525/I-33, 83-95, 1995 (in Japanese).

(Received September 6, 1996)